IEEE Access
Multidisciplinary | Rapid Review | Open Access Journal

Received May 29, 2019, accepted June 12, 2019, date of publication June 19, 2019, date of current version July 10, 2019.

Digital Object Identifier 10.1109/ACCESS.2019.2923672

Design of a LP, RHCP and LHCP Polarization-Reconfigurable Holographic Antenna

MEI LI[1,2], (Member, IEEE), MING-CHUN TANG[1], (Senior Member, IEEE), AND SHAOQIU XIAO[3], (Member, IEEE)

[1]Key Laboratory of Dependable Service Computing in Cyber Physical Society, Ministry of Education, School of Microelectronics and Communication Engineering, Chongqing University, Chongqing 400044, China
[2]State Key Laboratory of Millimeter Waves, Nanjing 210096, China
[3]School of Physics, University of Electronic Science and Technology of China, Chengdu 610054, China

Corresponding author: Mei Li (li.mei@cqu.edu.cn)

This work was supported in part by the National Natural Science Foundation of China under Contract 61701052, in part by the Young Backbone Teachers in Colleges and Universities of Chongqing under Contract 0307001104102, in part by the Opening Subject of State Key Laboratory of Millimeter Waves under Contract K202004, and in part by the Fundamental Research Funds for the Central Universities under Contract 2019CDXYTX0023.

ABSTRACT In this paper, the feasibility of utilizing the microwave hologram to realize the high-gain radiation with polarization agility performance is investigated, and an effective method to design the polarization-reconfigurable holographic antenna is presented. By utilizing a polarization-insensitive hologram as the leaky-wave radiating structure and an appropriately designed, embedded, polarization-reconfigurable feeding launcher to control the polarization state of the radiating leaky waves, a polarization-reconfigurable holographic antenna with broadside radiation and linearly polarized (LP), right-hand circularly polarized (RHCP), and left-hand circularly polarized (LHCP) polarization diversity is successfully achieved. The simulation results demonstrate that the proposed antenna exhibits pencil beams with aperture efficiency up to 28.3% for the three polarization states. Meanwhile, the stable gain performance with peak gain above 17.5 dBi and gain fluctuation less than 1.7 dB is obtained for the three reconfigurable polarization states. For verification, a prototype was fabricated and tested to validate the proposed design concept. Moreover, the working mechanism is investigated.

INDEX TERMS Reconfigurable antennas, polarization reconfigurable antennas, holographic antennas, metasurfaces, leaky-wave antennas.

I. INTRODUCTION

Holographic antennas are a kind of leaky-wave antennas, which are created using the interference pattern, *i.e.*, hologram, between the expected bound surface wave and the desired outgoing field. In practice, the holograms are usually constructed by a series of modulated conducting strips [1]–[3] or sub-wavelength, electrically small periodic unit cells [4]. Holographic antennas have the advantages of planar configuration, low cost, light weight, and conformability, as well as radiation performance of high gain and low loss, and thereby can be utilized in applications like satellite communication scenarios [5]. Various types of holographic antennas have been reported in the last decade. A 1-D linear polarization (LP) holographic antenna whose beam-width is squeezed in the *E*-plane was proposed in [6]. In order to realize pencil beams with high resolution, 2-D planar holographic antennas have gained increasing attention. Both LP and circular polarization (CP) holographic antennas have been proposed by implementing modulated scalar or tensor metasurfaces [7]–[11]. Furthermore, in order to make the holographic antennas versatile to meet different application situations, multi-function holographic antennas have been studied. A dual band holographic antenna was designed in [10] and a dual CP holographic antenna was theoretically and experimentally

The associate editor coordinating the review of this manuscript and approving it for publication was Kwok L. Chung.

This work is licensed under a Creative Commons Attribution 3.0 License. For more information, see http://creativecommons.org/licenses/by/3.0/

analyzed in [13], [14]. A polarization-diversity holographic antenna, which could realize LP or CP radiation by controlling the magnitude and phase of four excitation ports, was reported in [15]. Multi-beam holographic antennas were designed in [16], [17]. Besides, a holographic surface with CP focused near-field was presented in [18].

Polarization-reconfigurable antennas are capable of dynamically modifying their polarization states between different polarizations and thus share the merits of enhancing the system capacity, mitigating polarization mismatch and reducing channel interference. For example, the capability of switching between right-hand circular polarization (RHCP) and left-hand circular polarization (LHCP) can be used to increase the channel capacity in satellite communication systems [19]. Polarization-reconfigurable antennas are usually developed based on resonant-type antennas in the form of patch antennas or dipole antennas by loading PIN diodes on their feeding networks or radiating structures [20]–[26]. However, their directivity is relatively low, *i.e.*, generally less than 10dBi [21]–[25]. In order to meet the high gain requirement in some practical applications, antenna arrays constructed by those polarization-reconfigurable elements were utilized to further improve the directivity [27]–[29]. However, the array configuration would multiply the number of the loaded PIN diodes, which would inevitably cause severe processing complexity and insertion loss. As an alternative, holographic antenna with the inherent advantages of high gain and low loss could be attractive to be adopted as the basic radiating structure to design high gain polarization-reconfigurable antenna.

However, even though various holographic antennas have been reported, there are few references on electrically-controlled polarization-reconfigurable holographic antennas. The difficulty in realizing a pencil-beam polarization-reconfigurable holographic antenna lies in two main aspects: Firstly, different holograms consisting of different patterns of sub-wavelength metallic pixels are usually required to effectively generate a desired leaky wave with LP or CP radiation state [4], [8]. Nevertheless, it would be very complicated to alter the hologram pattern by loading plenty of PIN diodes on its thousands of sub-wavelength pixels. Secondly, the issue of integrating a compact feeding launcher as well as PIN bias circuits should be addressed.

In this paper, we propose a polarization-reconfigurable holographic antenna, which could switch its polarization state between LP, RHCP and LHCP by simply utilizing four PIN diodes. The aforementioned problem is solved by employing a polarization-insensitive surface-wave waveguide (SWG) to construct the hologram. It is known that an arbitrary polarization could be decomposed into a TE mode and a TM mode and polarization-insensitive SWG could support TE and TM modes with the same phase velocity [30]. Therefore, a polarization-insensitive SWG exhibits the same electromagnetic propagation property regardless of the polarization states of the excited waves. The proposed polarization-reconfigurable holographic antenna consists of a polarization-insensitive hologram as the radiating structure and an embedded polarization-reconfigurable feeding launcher. There are two appealing advantages accompanied with such design. On the one hand, since the polarization-insensitive hologram can support both TE and TM modes with the same phase velocity, the feeding launcher could fully illuminate the whole hologram no matter what polarized waves are excited. Therefore, the proposed antenna radiates rotationally symmetric beams with a relatively high aperture efficiency. On the other hand, in contrast to array-type polarization-reconfigurable antennas, the proposed antenna can reconfigure three polarization states with high directivity by switching only four PIN diodes, which are loaded on the embedded feeding launcher, and therefore the biasing issues and processing complexity are dramatically reduced.

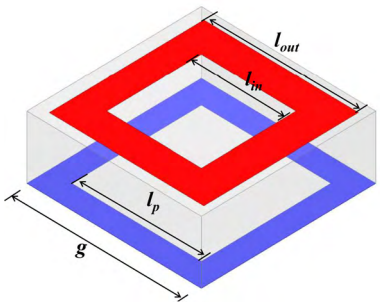

FIGURE 1. Loop-wire unit cell structure.

II. ANTENNA DESIGN

A. POLARIZATION-INSENSITIVE HOLOGRAM DESIGN

Polarization-insensitive SWG composed by loop-wire unit cells [30] is utilized to synthesize the desired polarization-insensitive hologram. Fig. 1 shows the configuration of the loop-wire unit cell. A metallic square loop and a metallic wire-grid are printed on the two faces of a single-layer 1.575 mm-thick Rogers RT/duroid 5880 substrate with relative permittivity of $\varepsilon_r = 2.2$. The square lattice constant of the unit cell is $g = 3.5$ mm. The outer edge length of the square ring is kept as a constant of $l_{out} = 3.3$mm. The inner edge lengths of the square ring and the wire-grid are l_{in} and l_p, respectively. When selecting appropriate values of l_{in} and l_p, the dispersion curves of the TM mode and TE mode would overlap at a certain frequency, which means TM mode and TE mode have the same phase velocity, exhibiting the polarization-insensitive property. Fig. 2 plots the dispersion diagram of the loop-wire unit cell when choosing $(l_{in}, l_p) =$ (2.6 mm, 1.9 mm). As is shown in Fig. 2, the TM mode and TE mode exhibit the same wave number ($\beta_{\mathrm{TM}} = \beta_{\mathrm{TE}} = 1.28\ k_0$, where k_0 is the wavenumber in the free space) at 15GHz. Therefore, the effective refractive indexes of the TM mode and TE mode are the same ($n_{\mathrm{TM}} = n_{\mathrm{TE}} = 1.28$) at 15GHz when setting $(l_{in}, l_p) = (2.6$ mm, 1.9 mm). The dispersion curves of the bare substrate,*i.e.*, without the loaded loops, were also plotted in Fig. 2 as a reference.

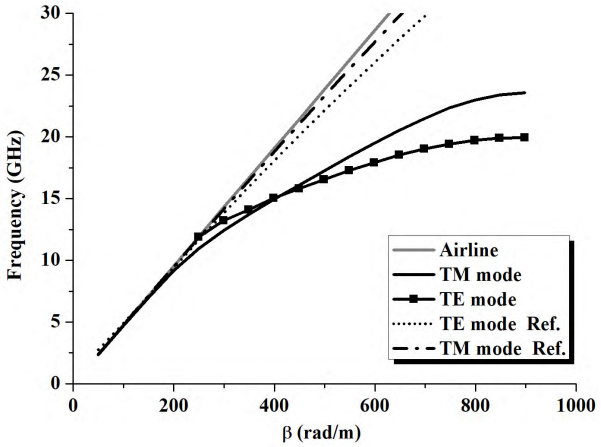

FIGURE 2. Dispersion curve of the loop-wire SWG when setting $(l_{in}, l_p) = (2.6\text{ mm}, 1.9\text{ mm})$.

It is demonstrated that the dispersion curves of both the loop-wire structure and the bare substrate structure are below the light line, manifesting the surface-wave characteristics. Besides, it is noticed that the dispersion curves of the bare substrate are close to the light line, which means the surface waves are weakly bound to the structure. On the contrast, the dispersion curves of the loop-wire structure are bend away from the light line as frequency increases, indicating the waves are tightly bound to the loop-wire structure. Therefore, the loop-wire cells could serve as a good polarization-insensitive SWG. A series of indexes satisfying $n_{\mathrm{TM}} = n_{\mathrm{TE}}$ at the operation frequency of 15GHz can be obtained when selecting different sets of (l_{in}, l_p). Following the same design process as in [9], the values of l_{in} and l_p can be uniquely determined for a given index n by solving the following two polynomial fitting functions, which are as follows:

$$n = 2.3759 - 1.23331\, l_{in} + 0.31207\, l_{in}^2 \quad (1)$$

$$n = 2.3759 - 1.23331\, l_p + 0.31207\, l_p^2 \quad (2)$$

A hologram with broadside radiation could be synthesized based on our previous developed modulation principle in terms of effective refractive index [9]. The modulation function is as follows:

$$n = X + M\ cos(Xk_0\rho) \quad (3)$$

where X represents the average refractive index, M is the modulation depth and ρ is the radial distance from the center point in a cylindrical coordinate system.

According to formulas (1), (2) and (3), a polarization-insensitive hologram constituted by loop-wire unit cells could be synthesized. Fig. 3 shows the designed polarization-insensitive hologram when setting $X = 1.3$, $M = 0.13$, and $\rho \leq 43$mm. Note that both the top face and the bottom face of the single-layer hologram constructed by the loop-wire unit cells are sinusoidally modulated, as is shown in Fig. 3(a) and (b).

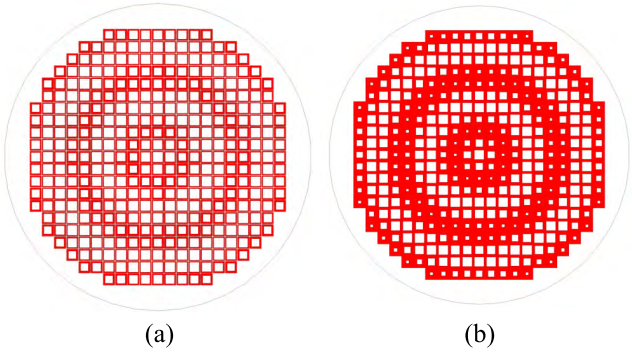

FIGURE 3. Polarization-insensitive hologram composed of loop-wire unit cells in square lattice. (a) Top face pattern. (b) Bottom face pattern.

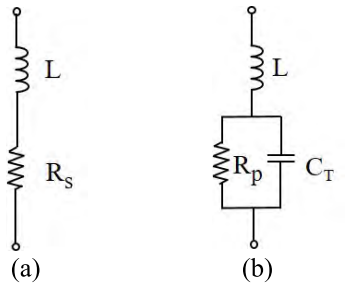

FIGURE 4. Equivalent circuit of a PIN diode. (a) ON state. (b) OFF state. L is package inductance, R_S is the series resistance under forward bias, C_T is the total capacitance at reverse bias, and R_p is the reverse parallel resistance.

B. POLARIZATION-RECONFIGURABLE HOLOGRAPHIC ANTENNA DESIGN

A polarization-reconfigurable holographic antenna by integrating the polarization-insensitive hologram with a polarization-reconfigurable feeding launcher is designed in this Section. The polarization-reconfigurable feeding launcher is capable of reconfiguring LP, RHCP and LHCP polarization states by using electrically-controlled switches. Here, PIN diodes are utilized as switches to modifying the polarization states by changing the bias conditions. The equivalent circuits of a PIN diode in forward-bias condition, or ON, and reverse-bias condition, or OFF, are illustrated in Fig. 4 [31]. In microwave ranges, the resistance of the package inductance L is usually negligible compared with the series resistance R_s at ON state and the reverse parallel resistance R_p is negligible compared with the resistance introduced by the total capacitance C_T at OFF state. Therefore, in simulation, PIN diodes are commonly represented by a small resistor of R_s at ON state and a small capacitor of C_T at OFF state. In this paper, four MA4GP907 PIN diodes [32] with $R_s = 4.2\ \Omega$ and $C_T = 0.025$ pF are utilized to implement the reconfigurability.

The configuration of the proposed polarization-reconfigurable holographic antenna is depicted in Fig. 5. As is shown in Fig. 5(a), the antenna consists of two circular substrate layers (Layer1 and Layer2) with radius of 43mm. The two substrate layers are using Rogers RT/duroid 5880 material with

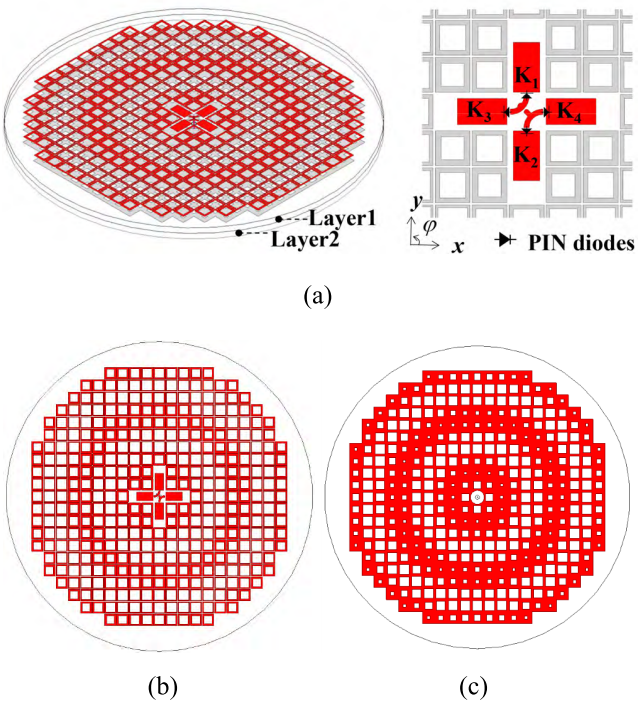

FIGURE 5. Configuration of the proposed polarization-reconfigurable holographic antenna. (a) 3-D view. The outer conductor of the SMA probe is soldered to the ground. $l_1 = 4.7$mm, $w_1 = 2.5$mm, $R_1 = 1.75$mm and $R_2 = 1.25$mm. (b) Top view of Layer1. (c) Bottom view of Layer1.

the relative dielectric constant of $\varepsilon_r = 2.2$ and a thickness of $h_1 = h_2 = 1.575$mm. The Layer1 is developed from the polarization-insensitive hologram that is shown in Fig. 3 by integrating the PIN loaded polarization-reconfigurable feeding launcher. It is obvious that the polarization-insensitive hologram exhibits bidirectional radiation with beams pointing to forward ($\theta = 0°$) and backward direction ($\theta = 180°$). In order to achieve unidirectional radiation, the hologram is backed by a grounded substrate, *i.e.*, Layer2.

In order to effectively couple the near field electromagnetic waves to the polarization-insensitive hologram, an appropriate polarization-reconfigurable feeding launcher is desired. In the literature, different types of feeding launchers have been utilized to feed leaky-wave antennas [33], [34]. Here, based on the specific hologram configuration with loop-wire cells arranged in square lattice, a properly designed, 50Ω SMA fed, cross-dipole-type feeding launcher is integrated on Layer1, as is depicted in Fig. 5 (a). The cross-dipole is divided into two pairs with one connected to the inner conductor of the SMA probe and the other connected to the outer conductor. The detailed geometry of the hologram integrated with the polarization-reconfigurable feeding launcher is shown in Figs. 5 (b) and (c). There is a circular slot with radius of $R_s = 2$mm etched in the center of the bottom face of the Layer1 substrate to isolate the SMA probe, as is shown in Fig. 5(c). Four PIN diodes with $R_s = 4.2\ \Omega$ and $C_T = 0.025$ pF are inserted into the four slots etched in the four arms of the cross dipole. By switching the

TABLE 1. LP, RHCP and LHCP reconfigurability by modifying pin states.

K_1	K_2	K_3	K_4	Pol. State
OFF	OFF	OFF	OFF	**LP**
OFF	OFF	ON	ON	**RHCP**
ON	ON	OFF	OFF	**LHCP**

ON and OFF state of the four PIN diodes (K_1, K_2, K_3 and K_4), the cross-dipole could operate in three reconfigurable polarization states, *i.e.*, LP, RHCP and LHCP states. The feasibility of using cross-dipole to achieve LP and CP reconfigurability has been reported [24], [35]. Correspondingly, the holographic antenna could realize three switchable polarization states by adjusting the ON and OFF state of the four PIN diodes. In details, when the four PIN diodes operate in the OFF state, the holographic antenna exhibits LP radiation with polarization parallel to the $\phi = 135°$ direction. When PIN diodes K_1, K_2 operate in the OFF (ON) state and K_3, K_4 operate in the ON (OFF) state, the holographic antenna operates in the RHCP (LHCP) state. The polarization reconfigurability of the holographic antenna is summarized in Table 1.

C. BIAS CIRCUITS DESIGN

Fig. 6(a) depicts the overall antenna configuration integrated with the bias circuits. A metallic cavity with a wall height of 2mm is utilized for mechanical installation convenience. In order to print the low-pass filters, which are required by the DC-bias circuits to block RF currents, the grounded substrate Layer2 is divided into two RT/duroid 5880 substrates, *i.e.*, Layer2_1 and Layer2_2, with a thickness of 0.787mm, which is of half height of the Layer2. Fig. 6 (b) shows the detailed configuration of the bias circuits to control the ON and OFF states of the four PIN diodes. One end of the four PIN diodes is electrically connected to the DC bias lines (V_{01}, V_{02}, V_{11}, V_{12}) and the other end is electrically connected to the inner (outer) conductor of the SMA probe. A DC biasing module composed by a low-pass filter is shown in Fig. 6 (c), which is printed on a grounded RT/duroid 5880 substrate with a thickness of 0.787mm. By connecting one port of the DC biasing module to the SMA probe, the SMA probe's inner and outer conductor are electrically controlled by V_1 and V_0, respectively. Therefore, four PIN diodes can be individually switched into OFF or ON state by controlling the DC voltage pairs (V_0, V_{01}), (V_0, V_{02}) and (V_1, V_{11}), (V_1, V_{12}). Notice that the low-pass filters composed by sectors with radian of $\pi/3$ are utilized to block RF currents. The detailed geometry of the cross-dipole launcher is illustrated in Fig. 6(c) and the specific parameter values are provided in Table 2.

D. SIMULATION RESULTS

The performance characteristics of the proposed polarization-reconfigurable holographic antenna were investigated using Ansoft HFSS. The reflection coefficients in different polarization states are shown in Fig. 7. It is manifested that the proposed antenna maintains good impedance matching,

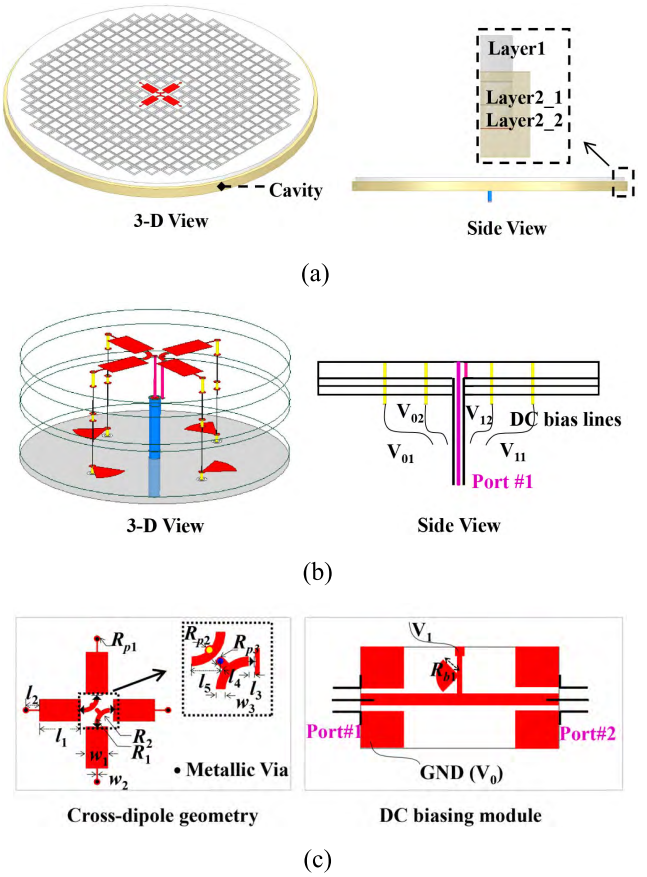

FIGURE 6. Configuration of the polarization-reconfigurable antenna. (a) Polarization-reconfigurable holographic antenna integrated with the bias circuits. (b) 3-D isometric view and side view of the feeding launcher integrated with bias circuits. (c) The detailed geometry of the cross-dipole type launcher and the DC biasing module printed on a 50Ω CPW transmission line.

TABLE 2. Parameter values of the antenna configuration (unit: mm).

l_1	l_2	l_3	l_4	l_5	w_1	w_2
4.7	1.525	0.3	0.39	1.55	2.5	0.15
w_3	R_1	R_2	R_{p1}	R_{p2}	R_{p3}	R_{b2}
0.5	1.75	1.25	0.35	0.3	0.235	3.6

i.e., $|S_{11}| < -10$dB, over the frequency range from 14.58GHz to 15.80GHz (fractional bandwidth of 8%) for LP, RHCP and LHCP states. Note that, due to the symmetric configuration for RHCP and LHCP operation, the antenna exhibits the same performance for the RHCP and LHCP states.

The radiation patterns of the proposed polarization-reconfigurable holographic antenna operating in LP and RHCP states at 15GHz are plotted in Fig. 8. The result for LHCP state is omitted, due to the exactly same pattern as for RHCP state in theory. As is shown in Fig. 8, the antenna exhibits pencil beams with the same beam-width in the E-plane and H-plane radiation patterns under the LP operation (in the XZ- and YZ-plane under the RHCP polarization).

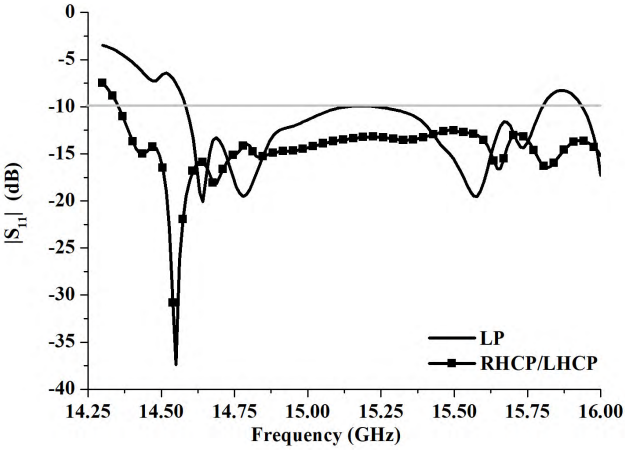

FIGURE 7. Reflection coefficients of the proposed antenna when operating in LP, RHCP and LHCP states.

The realized broadside gain of the proposed antenna is 17.34 dBi in the LP state and 17.31 dBic in the RHCP state at 15GHz. Accordingly, the aperture efficiency η (calculated by $\eta = \frac{G\lambda^2}{4\pi A_{area}}$, where G is the gain and A_{area} is the physical size of the holographic antenna) is about 28.3% for both the LP and CP polarization states. It is worth mentioning that typical values of the aperture efficiency of planar holographic antennas range between 0% and 20%, due to their leaky wave nature [7]. It is possible to further increase the aperture efficiency by imposing tapered modulation on the hologram [36], [37].

The broadside realized gain and axial ratio (AR) versus frequency for the LP, RHCP and LHCP states are shown in Fig. 9. As is seen from Fig. 9, the realized gain ranges from 16.17dBi to 17.75dBi over the bandwidth of 14.7-15.55GHz for the LP state, and ranges from 15.90dBic to 17.59dBic for the RHCP and LHCP states. The gain fluctuation is less than 1.7dB over the bandwidth of 14.7-15.55GHz for the three reconfigurable polarizations. Therefore, the gain curves for the LP, RHCP and LHCP states are consistent with each other. In addition, the antenna maintains good AR values (*i.e.*, < 3dB) over the overlapped bandwidth of 14.76-15.55GHz (5.2%). Besides, the proposed holographic antenna exhibits low loss property. According to our simulation study, the radiation efficiency e, which is calculated by $e = \frac{P_{rad}}{P_{acc}}$, *i.e.*, the ratio of the radiated power to the accepted power, is 98% and 96% for the LP and CP polarization at 15GHz, respectively. When the port return loss is taken into account, *i.e.*, the radiation efficiency calculated by $e = \frac{P_{rad}}{P_{in}}$, the corresponding radiation efficiency is 91% and 92% for the LP and CP, respectively. Note that, all the losses have been considered in the simulation.

III. EXPERIMENT AND OPERATION MECHANISM ANALYSIS

A polarization-reconfigurable holographic antenna with integrated DC bias circuits was fabricated and experimentally

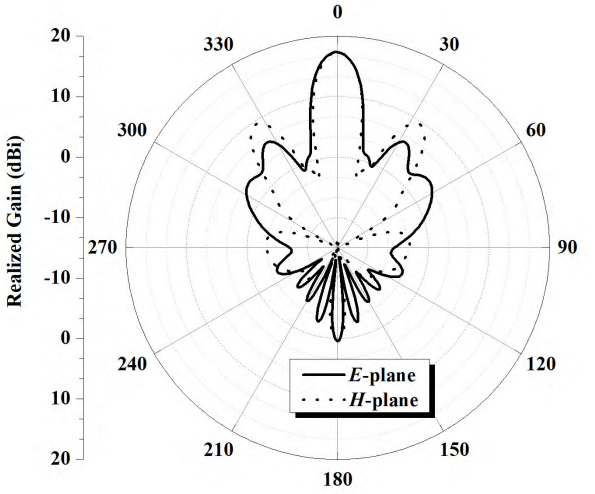

(a)

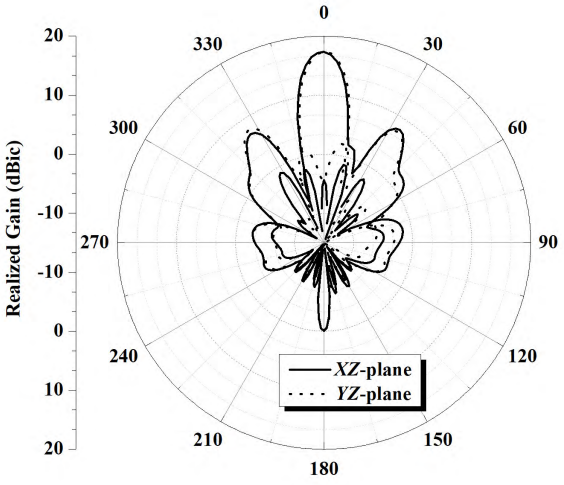

(b)

FIGURE 8. Radiation patterns of the proposed antenna at 15GHz. (a) E- and H-plane patterns operating in LP state. (b) XZ- and YZ-plane patterns operating in the RHCP state.

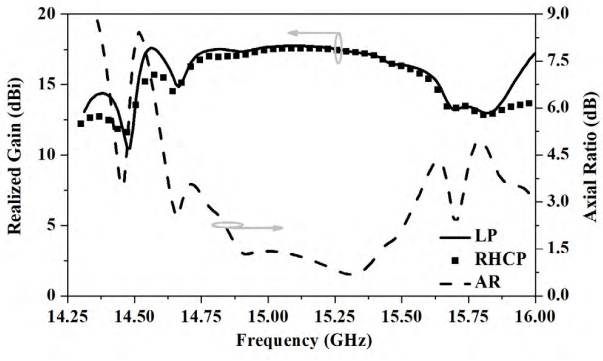

FIGURE 9. Realized broadside gain for LP, RHCP, and LHCP states and AR for the RHCP and LHCP states.

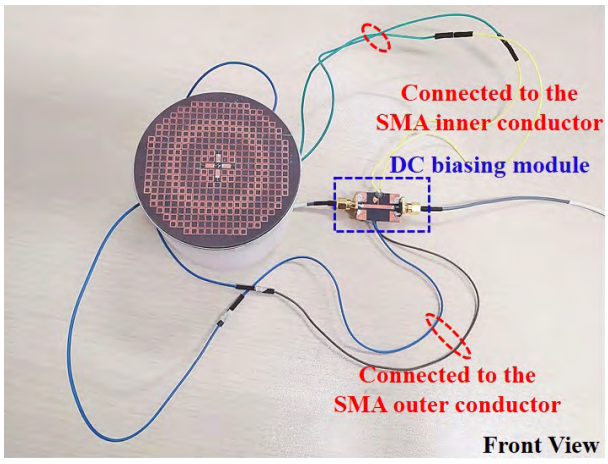

(a)

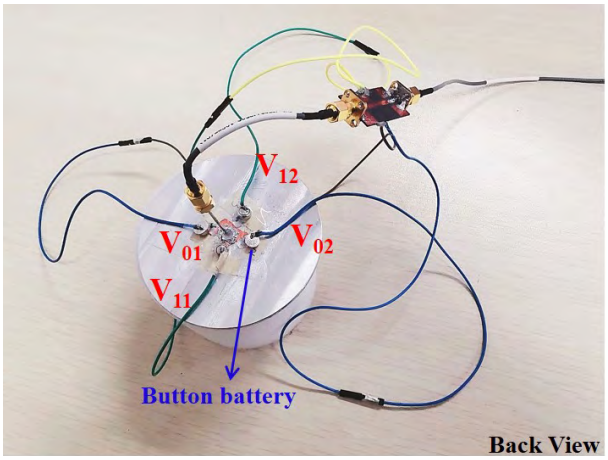

(b)

FIGURE 10. Fabricated prototype of the polarization-reconfigurable holographic antenna connected with the DC bias circuits. (a) Front view. (b) Back view.

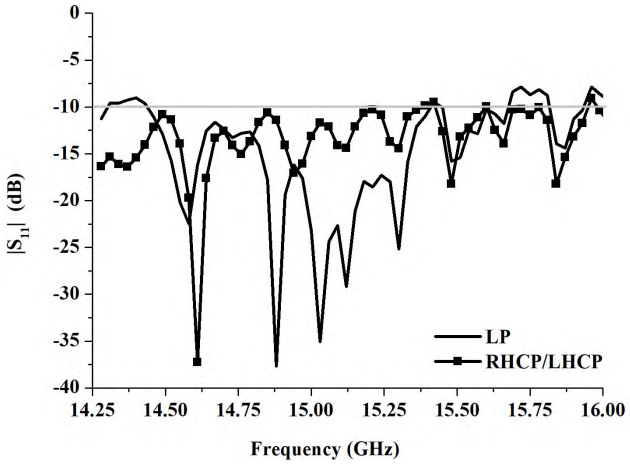

FIGURE 11. Measured reflection coefficients of the fabricated polarization-reconfigurable holographic antenna.

studied. The prototype is shown in Fig. 10. Four button batteries are used as the DC sources to control the ON/OFF states of the four loaded PIN diodes.

The measured reflection coefficients of the fabricated antenna are shown in Fig. 11. It is manifested that the antenna maintains good impedance matching, *i.e.*, $|S_{11}|$ <-10dB,

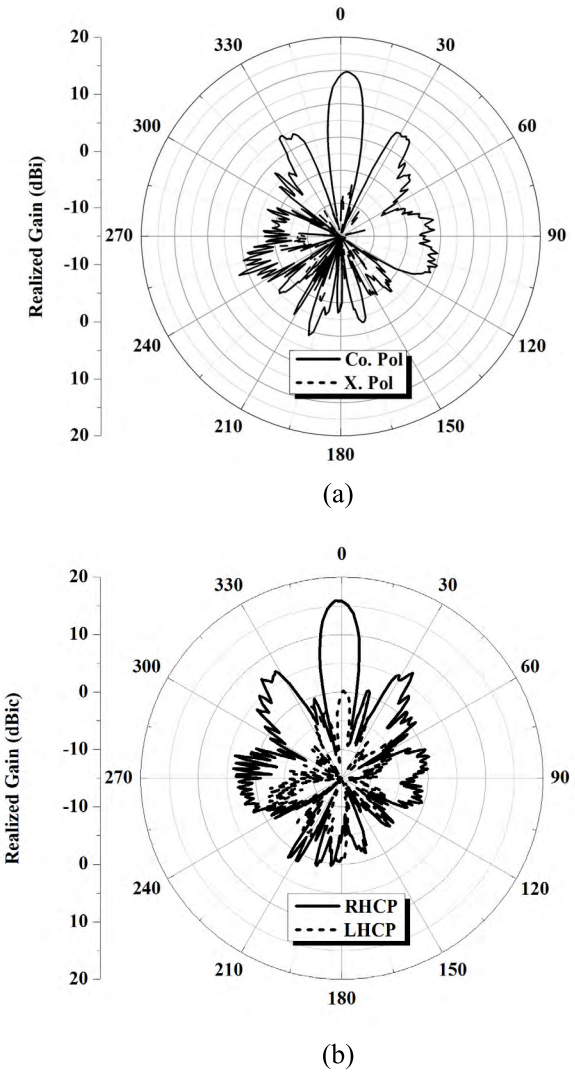

FIGURE 12. Measured radiation patterns of the fabricated antenna at 14.6GHz. (a) H-plane pattern operating in LP state. (a) YZ-plane pattern operating in the RHCP state.

over the frequency range from 14.5GHz to 15.65GHz for LP, RHCP and LHCP states. Note that the DC biasing module is not taken into account in the simulation, which may cause differences between the measured and simulated reflection coefficients. The radiation patterns were measured in a far-field anechoic chamber. Fig. 12 shows the measured patterns when the antenna operates in the LP and RHCP polarization states. The measured maximum gain is 15.9dBic for the RHCP operation at 14.6GHz. The measured maximum gain is 15.8dBi for the LP operation. Accordingly, the measured aperture efficiency is as high as 22.5%. Besides, the measured gain fluctuation is less than 2dB and 2.8dB over the bandwidth of 14.5GHz-15.65GHz for the LP and RHCP, respectively. Compared with patterns shown in Fig. 9, consistent patterns were observed as shown in Fig. 12.

The comparisons among the reported referenced antennas and the proposed polarization-reconfigurable holographic antenna are shown in Table 3. As is demonstrated

TABLE 3. Comparison of the proposed antenna with the referenced antennas.

Work	f_0 (GHz)	G_{max} (dBi)	Polarization	Electrically controlled	No. of PIN diodes
[3]	60	21.82[1]	LP	No	-
[7]	12	14.8[1]	LP or CP	No	-
[13]	13.5	25[1]	Dual CP	No	-
[14]	13.4	26.6[2]	Dual CP	No	-
[26]	5	11.2[2]	LP/RHCP/LHCP	Yes	8
[27]	2.4	13.5[2]	Dual LP	Yes	16
This work	15	17.75[1] 15.9[2]	LP/RHCP/LHCP	Yes	4

[1] denotes the simulated maximum gain and [2] denotes the measured maximum gain.

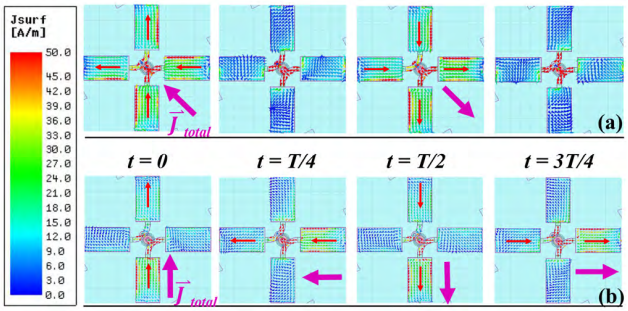

FIGURE 13. Current distributions on the cross-dipole structures at 15GHz under different polarization states. (a) 135° LP. (b) RHCP. T represents one period.

in Table 3, holographic antennas are capable of obtaining the admirable high directivity performance, while their polarization diversity property is difficult to be electrically controlled [3], [7], [13], [14]. For array-type polarization-reconfigurable antennas, the number of PIN diodes are increased to obtain a higher directivity [24], [27]. To sum up, the proposed antenna figures both high directivity and LP, RHCP and LHCP reconfigurability with the requirement of only four PIN diodes.

Since the polarization-insensitive hologram is capable of maintaining the polarization states of the excited waves, which are determined by the feeding launcher. The polarization-reconfigurable operation mechanism of the proposed antenna could be explained by investigating the current distributions excited on the cross dipole. Fig. 13 (a) and (b) illustrate the current distributions when the cross dipole operates at LP and RHCP, respectively. Notice that Fig. 13 shows the case without hologram presence. As is indicated in Fig. 13 (a), when all the PIN diodes operate in the OFF state, the currents on the two dipoles oscillate synchronously, and the orientation of the resultant current vector parallel to azimuth angle of $\varphi = 135°$ direction, resulting in a 135° LP radiation state. In contrast, when the PIN diodes K_1 and K_2 operate in the OFF state, and K_3 and K_4 operate in the ON state, the current distributions on the two dipoles differ greatly in both magnitude and phase. It is shown in Fig. 13 (b) that the current on the dipole along the y axis reaches the maximum at $t = 0$, while that on the dipole

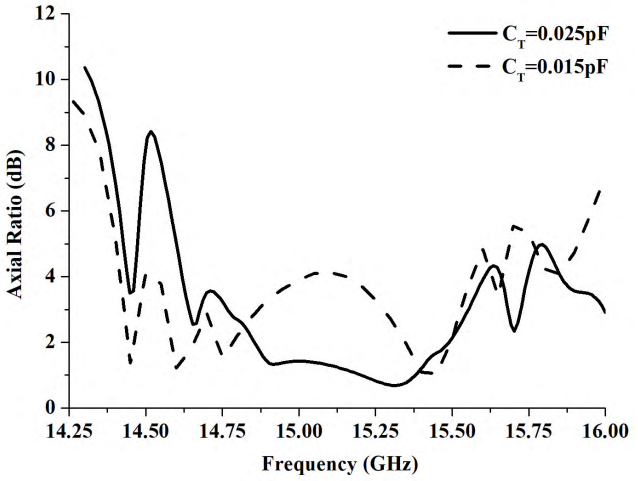

FIGURE 14. The effect of the capacitance C_T on the AR of the RHCP and LHCP operation states.

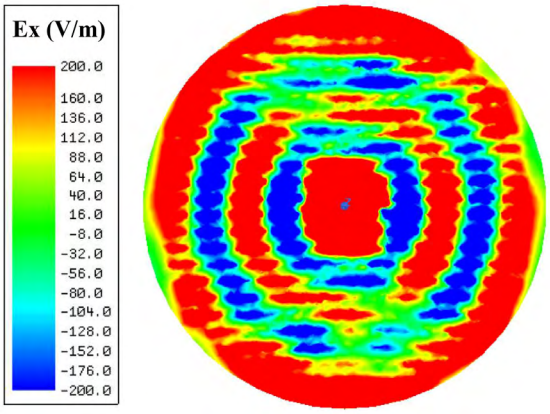

FIGURE 15. *Ex*-component distributions in the RHCP state at t = 0. The observation plane is at a distance of 1mm above the hologram surface.

along the x axis reaches the minimum, manifesting a 90° phase delay for the Ex and Ey components. According to Fig. 13 (b), the orientation of the resultant current rotates anticlockwise over the entire period, manifesting a RHCP operation. It should be noticed that, the equivalent capacitance C_T of the PIN diodes operating in the OFF state, *i.e.*, 0.025pF, is of great significant to the well-behaved RHCP or LHCP operation of the optimized antenna, which results in the required 90° phase delay between the two dipoles to achieve RHCP or LHCP performance. The effect of the capacitance C_T on the AR performance of the CP of the proposed holographic antenna is parametrically studied. As can be seen from Fig. 14, the AR value of the CP is increased from the original 1.4dB to 3.9dB at 15GHz when the C_T is 0.015pF.

As a demonstration that the polarization-insensitive hologram could be fully illuminated by the feeding launcher, Ex field distributions in the RHCP state at $t = 0$ is plotted in Fig. 15. As expected, waves coupled from the launcher propagate along the ratio direction and the whole hologram aperture is well illuminated, resulting in radiation patterns with a rotationally symmetric beam.

IV. CONCLUSION

The concept of integrating a polarization-insensitive hologram with a polarization-reconfigurable feeding launcher to accomplish a polarization-reconfigurable holographic antenna is proposed in this paper. For verification, a broadside, polarization-reconfigurable, holographic antenna with LP, RHCP, and LHCP polarization diversity performance is designed. The antenna consists of an embedded, compact, cross-dipole-type feeding launcher, which could reconfigure among LP, RHCP and LHCP states by utilizing four PIN diodes, and a polarization-insensitive, periodically modulated hologram, which could transform the coupled waves exited by the polarization-reconfigurable feeding launcher into leaky waves with main beam pointing to the broadside. Benefitting from the polarization-insensitive property, the hologram could maintain the polarization states of the excited electromagnetic waves, which are determined by the feeding launcher. Therefore, the proposed antenna presents a unique polarization-reconfigurable property, which makes it a good candidate in many practical applications like satellite communication systems and base station networks.

REFERENCES

[1] F. Caminita, M. Nannetti, and S. Maci, "Holographic surfaces realized by curvilinear strip gratings," in *Proc. 2nd Eur. Conf. Antennas Propag. (EuCAP)*, Nov. 2007, pp. 1–4.

[2] A. M. Patel and A. Grbic, "A printed leaky-wave antenna based on a sinusoidally-modulated reactance surface," *IEEE Trans. Antennas Propag.*, vol. 59, no. 6, pp. 2087–2096, Jun. 2011.

[3] C. Rusch, J. SchÃdfer, H. Gulan, P. Pahl, and T. Zwick, "Holographic mmW-antennas with TE_0 and TM_0 surface wave launchers for frequency-scanning FMCW-radars," *IEEE Trans. Antennas Propag.*, vol. 63, no. 4, pp. 1603–1613, Apr. 2015.

[4] B. H. Fong, J. S. Colburn, J. J. Ottusch, J. L. Visher, and D. F. Sievenpiper, "Scalar and tensor holographic artificial impedance surfaces," *IEEE Trans. Antennas Propag.*, vol. 58, no. 10, pp. 3212–3221, Oct. 2010.

[5] G. Minatti, M. Faenzi, E. Martini, F. Caminita, P. De Vita, D. González-Ovejero, M. Sabbadini, and S. Maci, "Modulated metasurface antennas for space: Synthesis, analysis and realizations," *IEEE Trans. Antennas Propag.*, vol. 63, no. 4, pp. 1288–1300, Apr. 2015.

[6] A. A. Oliner and A. Hessel, "Guided waves on sinusoidally-modulated reactance surfaces," *IRE Trans. Antennas Propag.*, vol. 7, no. 5, pp. 201–208, Dec. 1959.

[7] S. Pandi, C. A. Balanis, and C. R. Birtcher, "Design of scalar impedance holographic metasurfaces for antenna beam formation with desired polarization," *IEEE Trans. Antennas Propag.*, vol. 63, no. 7, pp. 3016–3024, Jul. 2015.

[8] G. Minatti, F. Caminita, E. Martini, and S. Maci, "Flat optics for leaky-waves on modulated metasurfaces: Adiabatic floquet-wave analysis," *IEEE Trans. Antennas Propag.*, vol. 64, no. 9, pp. 3896–3906, Sep. 2016.

[9] M. Li, S.-Q. Xiao, and D. F. Sievenpiper, "Polarization-insensitive holographic surfaces with broadside radiation," *IEEE Trans. Antennas Propag.*, vol. 64, no. 12, pp. 5272–5280, Dec. 2016.

[10] U. Beaskoetxea, V. Pacheco-Peña, B. Orazbayev, T. Akalin, S. Maci, M. Navarro-Cía, and M. Beruete, "77-GHz high-gain Bull's-eye antenna with sinusoidal profile," *IEEE Antennas Wireless Propag. Lett.*, vol. 14, pp. 205–208, 2015.

[11] C. J. Vourch and T. D. Drysdale, "V-band 'Bull's eye' antenna for CubeSat applications," *IEEE Antennas Wireless Propag. Lett.*, vol. 13, pp. 1092–1095, 2014.

[12] Y. Li, A. Li, T. Cui, and D. F. Sievenpiper, "Multiwavelength multiplexing hologram designed using impedance metasurfaces," *IEEE Trans. Antennas Propag.*, vol. 66, no. 11, pp. 6408–6413, Nov. 2018.

[13] A. T. Pereda, F. Caminita, E. Martini, I. Ederra, J. C. Iriarte, R. Gonzalo, and S. Maci, "Dual circularly polarized broadside beam metasurface antenna," *IEEE Trans. Antennas Propag.*, vol. 64, no. 7, pp. 2944–2953, Jul. 2016.
[14] A. T. Pereda, F. Caminita, E. Martini, I. Ederra, J. Teniente, J. C. Iriarte, R. Gonzalo, and S. Maci, "Experimental validation of a Ku-band dual-circularly polarized metasurface antenna," *IEEE Trans. Antennas Propag.*, vol. 66, no. 3, pp. 1153–1159, Mar. 2018.
[15] D. Comite, S. K. Podilchak, P. Baccarelli, P. Burghignoli, A. Galli, A. P. Freundorfer, and Y. M. M. Antar, "Design of a polarization-diverse planar leaky-wave antenna for broadside radiation," *IEEE Access*, vol. 7, pp. 28672–28683, 2019.
[16] Y. B. Li, B. G. Cai, Q. Cheng, and T. J. Cui, "Isotropic holographic metasurfaces for dual-functional radiations without mutual interferences," *Adv. Funct. Mater.*, vol. 26, pp. 29–35, Jan. 2016.
[17] D. González-Ovejero, G. Minatti, G. Chattopadhyay, and S. Maci, "Multi-beam by metasurface antennas," *IEEE Trans. Antennas Propag.*, vol. 65, no. 6, pp. 2923–2930, Jun. 2017.
[18] J. L. Gómez-Tornero, D. Blanco, E. Rajo-Iglesias, and N. Llombart, "Holographic surface leaky-wave lenses with circularly-polarized focused near-fields—Part I: Concept, design and analysis theory," *IEEE Trans. Antennas Propag.*, vol. 61, no. 7, pp. 3475–3485, Jul. 2013.
[19] H. Wong, W. Lin, X. Wang, and M. Lu, "LP and CP polarization reconfigurable antennas for modern wireless applications," in *Proc. Int. Symp. Antennas Propag.*, Oct./Nov. 2017, pp. 1–2.
[20] S. Gao, A. Sambell, and S. S. Zhong, "Polarization-agile antennas," *IEEE Antennas Propag. Mag.*, vol. 48, no. 3, pp. 28–37, Jun. 2006.
[21] R.-H. Chen and J.-S. Row, "Single-fed microstrip patch antenna with switchable polarization," *IEEE Trans. Antennas Propag.*, vol. 56, no. 4, pp. 922–926, Apr. 2008.
[22] H. Sun and S. Sun, "A novel reconfigurable feeding network for quad-polarization agile antenna design," *IEEE Trans. Antenna Propag.*, vol. 64, no. 1, pp. 311–316, Jan. 2016.
[23] G.-W. Yang, J. Li, B. Cao, D. Wei, S.-G. Zhou, and J. Deng, "A compact reconfigurable microstrip antenna with multidirectional beam and multipolarization," *IEEE Trans. Antennas Propag.*, vol. 67, no. 2, pp. 1358–1363, Feb. 2019.
[24] H. H. Tran, N. N-Trong, T. T. Le, and H. C. Park, "Wideband and multi-polarization reconfigurable crossed bowtie dipole antenna," *IEEE Trans. Antennas Propag.*, vol. 65, no. 12, pp. 652–660, Dec. 2017.
[25] K. L. Chung, S. Xie, Y. Li, R. Liu, S. Ji, and C. Zhang, "A circular-polarization reconfigurable Meng-shaped patch antenna," *IEEE Access*, vol. 6, pp. 51419–51428, 2018.
[26] L.-Y. Ji, P.-Y. Qin, Y. J. Guo, C. Ding, G. Fu, and S.-X. Gong, "A wideband polarization reconfigurable antenna with partially reflective surface," *IEEE Trans. Antenna Propag.*, vol. 64, no. 10, pp. 4534–4538, Oct. 2016.
[27] W. Lin and H. Wong, "Polarization reconfigurable aperture-fed patch antenna and array," *IEEE Access*, vol. 4, pp. 1510–1517, 2016.
[28] J. Hu, Z.-C. Hao, and W. Hong, "Design of a wideband quad-polarization reconfigurable patch antenna array using a stacked structure," *IEEE Trans. Antenna Propag.*, vol. 65, no. 6, pp. 3014–3023, Jun. 2017.
[29] B. Feng, L. Li, Q. Zeng, and C.-Y.-D. Sim, "A low-profile metamaterial loaded antenna array with anti-interference and polarization reconfigurable characteristics," *IEEE Access*, vol. 6, pp. 35578–35589, 2018.
[30] M. Li, S. Xiao, J. Long, and D. F. Sievenpiper, "Surface waveguides supporting both TM mode and TE mode with the same phase velocity," *IEEE Trans. Antennas Propag.*, vol. 64, no. 9, pp. 3811–3819, Sep. 2016.
[31] J. Ardizzoni, "Driving PIN diodes: The op-amp alternative," Analog Dialogue, Tech. Rep. 44-02, Feb. 2010, pp. 1–5.
[32] *Data Sheet of MA4GP907 PIN Diodes*, MACOM Technol. Solutions (MA-Com), GaAs Flip Chip PIN, Rev. V6, 2011.
[33] M. Ettorre, S. Bruni, G. Gerini, A. Neto, N. Llombart, and S. Maci, "Sector PCS-EBG antenna for low-cost high-directivity applications," *IEEE Antennas Wireless Propag. Lett.*, vol. 6, pp. 537–539, 2007.
[34] D. Comite, P. Baccarelli, P. Burghignoli, and A. Galli, "Omnidirectional 2-D leaky-wave antennas with reconfigurable polarization," *IEEE Antennas Wireless Propag. Lett.*, vol. 16, pp. 2354–2357, 2017.
[35] W.-S. Yoon, S.-M. Han, J.-W. Baik, S. Pyo, J. Lee, and Y.-S. Kim, "Crossed dipole antenna with switchable circular polarisation sense," *Electron. Lett.*, vol. 45, no. 14, pp. 717–718, Jul. 2009.
[36] J. S. Colbum, D. F. Sievenpiper, B. H. Fong, J. J. Ottusch, J. L. Visher, and P. R. Herz, "Advances in artificial impedance surface conformal antennas," in *Proc. IEEE Antennas Propag. Soc. Int. Symp.*, Jun. 2007, pp. 3820–3823.
[37] G. Minatti, E. Martini, and S. Maci, "Efficiency of metasurface antennas," *IEEE Trans. Antennas Propag.*, vol. 65, no. 4, pp. 1532–1541, Apr. 2017.

MEI LI (S'15–M'16) received the B.S. degree in electronic information science and technology from the Chengdu University of Information Technology, Chengdu, China, in 2010, and the Ph.D. degree in radio physics from the University of Electronic Science and Technology of China, Chengdu, in 2016. From 2014 to 2016, she was a Visiting Graduate with the Applied Electromagnetics Research Group, University of California at San Diego, San Diego, CA, USA. She is currently an Assistant Professor with the School of Microelectronics and Communication Engineering, Chongqing University, China. Her research interests include metasurfaces, antennas, and arrays.

MING-CHUN TANG (S'12–M'13–SM'16) received the B.S. degree in physics from the Neijiang Normal University, Neijiang, China, in 2005, and the Ph.D. degree in radio physics from the University of Electronic Science and Technology of China (UESTC), in 2013. From 2011 to 2012, he was a Visiting Scholar with the Department of Electrical and Computer Engineering, The University of Arizona, Tucson, AZ, USA. He is currently a Professor with the School of Microelectronics and Communication Engineering, Chongqing University, China. His research interests include electrically small antennas, RF circuits, metamaterial designs, and their applications. He was a recipient of the Best Student Paper Award at the 2010 International Symposium on Signals, Systems and Electronics (ISSSE2010), Nanjing, China. His Ph.D. student received the Best Student Paper Award from the IEEE 7th Asia-Pacific Conference on Antennas and Propagation (2018 IEEE APCAP), Auckland, New Zealand. He is also the Founding Chair of the IEEE AP-S/MTT-S Joint Chongqing Chapter. He has also served on the review boards of many journals, including the IEEE TRANSACTIONS ON ANTENNAS AND PROPAGATION, IEEE TRANSACTIONS ON MICROWAVE THEORY AND TECHNIQUES, IEEE ANTENNAS AND WIRELESS PROPAGATION LETTERS, *IEEE Antennas and Propagation Magazine*, and IEEE MICROWAVE AND WIRELESS COMPONENTS LETTERS, and many international conferences as the General Chair, a TPC Member, a Session Organizer, and the Session Chair. He serves on the editorial boards of several journals, including the IEEE ACCESS, *IET Electronics Letters*, and *IET Microwaves, Antennas & Propagation*.

SHAOQIU XIAO (M'05) received the Ph.D. degree in electro-magnetic field and microwave technology from the University of Electronic Science and Technology of China (UESTC), Chengdu, China, in 2003. In 2004, he joined UESTC as an Assistant Professor. From 2004 to 2006, he was with the Wireless Communications Laboratory, National Institute of Information and Communications Technology of Japan (NICT), Singapore, as a Research Fellow with the focus on the planar antenna and smart antenna design and optimization. From 2006 to 2010, he was an Associate Professor with UESTC, where he is currently a Professor. He visited the École Normale Supérieure de Cachan, Paris, France, as a Senior Research Scholar, in 2015. His current research interests include planar antenna and phased array, computational electromagnetics, microwave passive circuits, and time reversal electromagnetics. He has authored/coauthored more than 240 technical journals, conference papers, books, and book chapters.